

## Recent results, status and prospects for the BESIII experiment

This content has been downloaded from IOPscience. Please scroll down to see the full text.

2015 J. Phys.: Conf. Ser. 631 012043

(<http://iopscience.iop.org/1742-6596/631/1/012043>)

View [the table of contents for this issue](#), or go to the [journal homepage](#) for more

Download details:

IP Address: 142.66.3.42

This content was downloaded on 16/09/2015 at 13:10

Please note that [terms and conditions apply](#).

# Recent results, status and prospects for the BESIII experiment

Isabella Garzia for the BESIII Collaboration

INFN-Sezione di Ferrara, via Saragat 1, 44122 Ferrara, Italy

E-mail: [garzia@fe.infn.it](mailto:garzia@fe.infn.it)

**Abstract.** We report the measurement of the asymmetry  $\mathcal{A}_{CP}$  of the branching fractions of  $D^0 \rightarrow K^- \pi^+$  in the  $CP$ -odd and  $CP$ -even eigenstates using a data sample of  $2.92 \text{ fb}^{-1}$  collected with the BESIII detector at the center-of-mass energy  $\sqrt{s} = 3.773 \text{ GeV}$ . With the measured  $\mathcal{A}_{CP}$ , the strong phase difference  $\delta_{K\pi}$  between the doubly Cabibbo-suppressed process  $\bar{D}^0 \rightarrow K^- \pi^+$  and the Cabibbo-favored process  $D^0 \rightarrow K^- \pi^+$  is extracted. Using world-average values of external parameters, we obtain the most precise measurement of  $\delta_{K\pi}$  to date:  $\cos \delta_{K\pi} = 1.02 \pm 0.11 \pm 0.06 \pm 0.01$ . The first and second uncertainties are statistical and systematic, respectively, while the third arises from external input. Based on the same data sample a preliminary results of the parameter  $y_{CP}$  in  $D^0 \bar{D}^0$  oscillation is obtained. Finally, a summary of the recent results from charmonium spectroscopy is reported. The high statistics accumulated at the  $Y(4260)$  and  $Y(4360)$  energies help us to understand the nature and the properties of the XYZ states.

## 1. Introduction

Mixing between  $K^0$  and  $\bar{K}^0$ ,  $B^0$  and  $\bar{B}^0$ , and  $B_s$  and  $\bar{B}_s$  is well established, and is well described by the Standard Model (SM) box diagrams containing up-type ( $u$ ,  $c$ ,  $t$ ) quarks. In contrast, the  $D^0 - \bar{D}^0$  mixing amplitude at short distances involves loop containing down-type ( $d$ ,  $s$ ,  $b$ ) quarks. The  $d$  and  $s$  box amplitudes are suppressed by the GIM mechanism [1], while the contribution from loops involving  $b$  quark is suppressed by the CKM factor [2, 3]. Therefore, the short-distance SM prediction is very small, of the order of  $10^{-6}$ , and the charm mixing is expected to be dominated by long-distance processes, consisting of non-perturbative terms, and thus difficult to estimate. The measure of the charm mixing parameters helps to obtain information on the size of the long-distance effects and to the possible presence of new physics. Many experiments in the past decades indicate the that  $D^0$  and  $\bar{D}^0$  do mix, and more recently, charm mixing is established by LHCb [4] and CDF [5].

Mixing of neutral mesons occurs when the flavor eigenstates differ from the mass eigenstates. The two mass eigenstates of the neutral  $D$  meson system,  $|D_{1,2}\rangle$ , with masses  $m_{1,2}$  and decay widths  $\Gamma_{1,2}$ , can be expressed as a linear combinations of the flavor eigenstates  $|D^0\rangle$  and  $|\bar{D}^0\rangle$ :  $|D_{1,2}\rangle = p|D^0\rangle + q|\bar{D}^0\rangle$ , with the  $p$  and  $q$  complex parameters satisfying the condition  $|p|^2 + |q|^2 = 1$ . Conventionally, the charm mixing is described by two dimensionless parameters:

$$x = 2 \frac{m_1 - m_2}{\Gamma_1 + \Gamma_2}, \quad y = \frac{\Gamma_1 - \Gamma_2}{\Gamma_1 + \Gamma_2}. \quad (1)$$



Using the conventions  $CP|D^0\rangle = |\bar{D}^0\rangle$  and  $CP|\bar{D}^0\rangle = -|D^0\rangle$ , we construct the  $CP$  eigenstates as  $|D_{CP\pm}\rangle \equiv \frac{|D^0\rangle \pm |\bar{D}^0\rangle}{\sqrt{2}}$ , so that we can define the parameter  $y_{CP}$  as the difference between the effective lifetime of  $D$  decays to  $CP$  eigenstates and flavor eigenstates. In the absence of direct  $CP$  violation, but allowing small indirect  $CP$  violation [6], we have

$$y_{CP} = \frac{1}{2} \left[ y \cos \phi \left( \left| \frac{q}{p} \right| + \left| \frac{p}{q} \right| \right) - x \sin \phi \left( \left| \frac{q}{p} \right| - \left| \frac{p}{q} \right| \right) \right], \quad (2)$$

where  $\phi$  is the weak phase characterizing the  $CP$  violation in the interference between mixing and decay. Note that if  $CP$  is conserved,  $|p/q| = 1$  and  $\phi = 0$ , and hence  $y_{CP} = y$ .

Most of our knowledge about  $D^0 - \bar{D}^0$  mixing comes from time-dependent analysis. In particular, a very precise determination of the size of the mixing is obtained from the studies of the time dependent decay rate of the wrong-size process  $D^0 \rightarrow K^+\pi^-$ , which are sensitive to the quantities  $y' = y \cos \delta_{K\pi} - x \sin \delta_{K\pi}$  and  $x' = x \cos \delta_{K\pi} + y \sin \delta_{K\pi}$  [4, 5, 7, 8]. The  $y'$  and  $x'$  "rotated" parameters depend on the the relative strong phase  $-\delta_{K\pi}$  between the doubly Cabibbo-suppressed (DCS) decay  $D^0 \rightarrow K^+\pi^-$  and the corresponding Cabibbo-favored (CF)  $\bar{D}^0 \rightarrow K^-\pi^+$ , and is defined as:

$$\frac{\langle K^-\pi^+ | \bar{D}^0 \rangle}{\langle K^-\pi^+ | D^0 \rangle} = -r e^{-i\delta_{K\pi}}, \quad (3)$$

where  $r = |\langle K^-\pi^+ | \bar{D}^0 \rangle| / |\langle K^-\pi^+ | D^0 \rangle|$ , and  $\delta_{K^-\pi^+} \equiv \delta_{K^+\pi^-}$  in the limit of  $CP$  conservation. A precise measurement of  $\delta_{K\pi}$  is, therefore, necessary to extract  $x$  and  $y$  from  $x'$  and  $y'$ , and helps to improve accuracy of the  $\gamma/\phi_3$  angle measurement in the CKM matrix.

In the first part of this report, we present the measurements of the strong phase  $\delta_{K\pi}$  and  $y_{CP}$  obtained from a time-independent analysis. We use a sample of  $2.92 \text{ fb}^{-1}$  of data collected at the center-of-mass energy  $\sqrt{s} = 3.773 \text{ GeV}$  in  $e^+e^-$  collisions with the BESIII detector [9], and we exploit the quantum-correlation in the mass-threshold production of the process  $e^+e^- \rightarrow D^0\bar{D}^0$ . In this process, the initial system has  $J^{PC} = 1^{--}$ , and so the  $D^0$  and  $\bar{D}^0$  mesons are in a  $CP$ -odd quantum-coherent state. Therefore, at any time, the two  $D$  mesons have opposite  $CP$ -eigenstates until one of them decays.

The second part of the report is dedicated to one of the main physics topics of the BESIII experiment: the charmonium spectroscopy. From 2009, a lot of data were taken in the energy region of about 4 GeV in order to study the  $X$ ,  $Y$ , and  $Z$  states recently observed in the charm mass region. These new states have properties that are not in agreement with the theoretical expectations for charmonium states, and they are so called charmonium-like state. There are a lot of interpretations in literature:  $c\bar{c}$  hybrids, glueballs, hadronic molecules, tetraquarks, etc., but more experimental informations are needed to reach a conclusion. In particular, in this report we summarize the latest results on the  $Z_c$  states.

## 2. The BESIII detector

The Beijing Spectrometer (BESIII) is a general purpose detector which covers 93% of the solid angle, and operates at the  $e^+e^-$  collider BEPCII. From the interaction point to the outside, BESIII is equipped with a main drift chamber (MDC) consisting of 43 layers of drift cells, a time-of-flight counter (TOF) with double-layer scintillators in the barrel and single-layer scintillator in the end-caps, an electromagnetic calorimeter (EMC) composed of 6240 CsI(Tl) crystals, a superconducting solenoid magnet providing a magnetic field of 1 T along the beam direction, and a muon counter (MUC) constituted by multi-layer resistive plate chambers installed in the steel flux-return yoke of the magnet. The spatial resolution achieved by the MDC is about  $135 \mu\text{m}$ , while the momentum resolution is 0.5% for charged particles with transverse momentum of

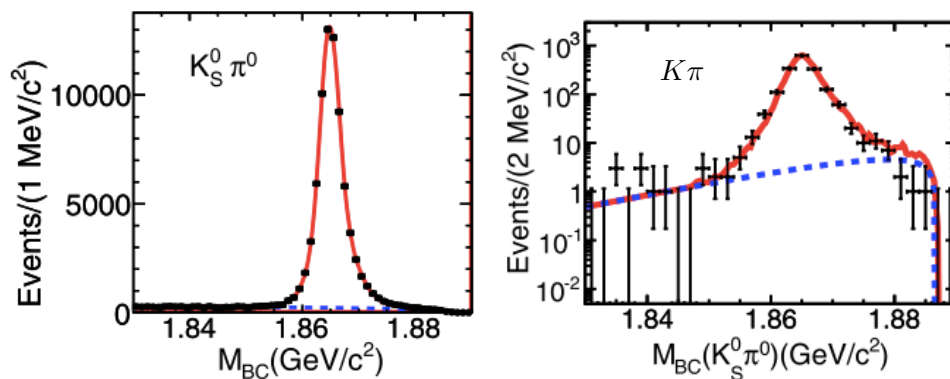


**Figure 1.** ST  $M_{BC}$  distribution of the  $D \rightarrow K_S^0 \pi^0$  final state (left), and DT  $M_{BC}$  distribution of the  $D \rightarrow K_S^0 \pi^0$  and  $D \rightarrow K^- \pi^+$  (right) final states. The red lines represent the fit to the distributions, while blue dashed lines the background contribution.

1 GeV/c. The EMC energy resolution for 1 GeV photon is 2.5% (5%) in the barrel (end-caps) region; the TOF time resolution is about 80 ps (110 ps) for the barrel (end-caps), and provides a  $K/\pi$  separation of  $2\sigma$  for momenta up to 1 GeV/c. More details can be found in Ref. [9].

### 3. Measurement of the relative strong phase $\delta_{K\pi}$

The relative strong phase can be accessed from [10, 11]

$$2r \cos \delta_{K\pi} + y = (1 + R_{WS}) \cdot \mathcal{A}_{CP}, \quad (4)$$

where  $R_{WS}$  is the decay ratio of the wrong-sign process  $\bar{D}^0 \rightarrow K^- \pi^+$  to the right-sign process  $D^0 \rightarrow K^- \pi^+$ , and

$$\mathcal{A}_{CP} \equiv \frac{\mathcal{B}_{D_{CP^-} \rightarrow K^- \pi^+} - \mathcal{B}_{D_{CP^+} \rightarrow K^- \pi^+}}{\mathcal{B}_{D_{CP^-} \rightarrow K^- \pi^+} + \mathcal{B}_{D_{CP^+} \rightarrow K^- \pi^+}} \quad (5)$$

is the asymmetry of  $CP$ -tagged  $D$  decay rates to  $K^- \pi^+$ . Using external parameters for  $r$ ,  $R_{WS}$ , and  $y$ , we can extract  $\delta_{K\pi}$  after the measurement of  $\mathcal{A}_{CP}$ . In particular, exploiting the quantum coherence, we use the  $D$ -tagging method to obtain the breaching fractions  $\mathcal{B}_{D_{CP^\pm} \rightarrow K\pi}$ :

$$\mathcal{B}_{D_{CP^\pm} \rightarrow K\pi} = \frac{n_{K\pi, CP^\pm}}{n_{CP^\pm}} \cdot \frac{\epsilon_{CP^\pm}}{\epsilon_{K\pi, CP^\pm}}, \quad (6)$$

where  $n_{CP^\pm}$  and  $\epsilon_{CP^\pm}$  are the yields and detection efficiencies of single tags (ST) of the  $CP^\pm$  final state, while  $n_{K\pi, CP^\pm}$  and  $\epsilon_{K\pi, CP^\pm}$  are the yields and detection efficiencies of double tag (DT) of the  $(CP^\pm, K\pi)$  final state, respectively.

In this analysis, we use 5  $CP$ -even  $D^0$  decay modes ( $K^+ K^-$ ,  $\pi^+ \pi^-$ ,  $K_S^0 \pi^0 \pi^0$ ,  $\pi^0 \pi^0$ ,  $\rho^0 \pi^0$ ), and 3  $CP$ -odd modes ( $K_S^0 \pi^0$ ,  $K_S^0 \eta$ ,  $K_S^0 \omega$ ), with  $\pi^0(\eta) \rightarrow \gamma\gamma$ ,  $K_S^0 \rightarrow \pi^+ \pi^-$  and  $\omega \rightarrow \pi^+ \pi^- \pi^0$ . The beam constrained mass  $M_{BC}$  and energy difference  $\Delta E$  are the two kinematic variables used to identify the signal:

$$M_{BC} \equiv \sqrt{E_D^2/c^2 - |\vec{p}_D|^2/c^2}, \quad \text{and} \quad \Delta E \equiv E_D - E_0, \quad (7)$$

where  $\vec{p}_D$  and  $E_D$  are the total momentum and energy of the  $D$  meson candidate, and  $E_0$  is the beam energy. Figure 1 shows the ST and DT  $M_{BC}$  distributions for one of the  $CP$ -odd final

state ( $D \rightarrow K_S^0 \pi^0$ ), for example. For each of the ST mode ( $CP+$  or  $CP-$ ), we construct the  $D \rightarrow K\pi$  among the unused charged tracks. The signal peaks at the nominal  $D^0$  mass, and we perform a maximum likelihood fit to the  $M_{BC}$  distributions in order to extract the yields. The signal shape is determined from MC simulation convoluted with a smearing Gaussian function, while the background is described by the ARGUS function. The fit results are shown in Fig. 1. Using Eq. (5), we measure  $\mathcal{A}_{CP} = (12.7 \pm 1.3 \pm 0.7)\%$ , where the uncertainties are statistical and systematic, respectively.

To extract the strong phase  $\delta_{K\pi}$  from Eq. 4, we quote the external input of  $r \equiv R_D = (3.47 \pm 0.06)\%$ ,  $y = (6.6 \pm 0.9)\%$  from HFAG [12], and  $R_{WS} = (3.80 \pm 0.05)\%$  from PDG [6], and we obtain [13]

$$\cos \delta_{K\pi} = 1.02 \pm 0.11 \pm 0.06 \pm 0.01. \quad (8)$$

The first uncertainty is statistical, the second is systematic, and the third is due to the external input parameters. This result is consistent with CLEO measurement [10] and provides the world best constrain on  $\delta_{K\pi}$ .

#### 4. Measurement of $y_{CP}$

The semileptonic branching fraction of the  $CP$ -eigenstates  $D_{CP\pm}$  can be written as  $\mathcal{B}_{D_{CP\pm} \rightarrow l} \sim \mathcal{B}_{D \rightarrow l}(1 \mp y_{CP})$ , where  $\mathcal{B}_{D \rightarrow l}$  denotes the branching fraction of the semileptonic  $D^0 \rightarrow hl\nu_l$  decay, which is independent of the  $CP$  eigenvalue of the parent  $D$  meson. Following Ref. [11],  $y_{CP}$  can be obtained as:

$$y_{CP} = \frac{1}{4} \left( \frac{\mathcal{B}_{D_{CP-} \rightarrow l}}{\mathcal{B}_{D_{CP+} \rightarrow l}} - \frac{\mathcal{B}_{D_{CP+} \rightarrow l}}{\mathcal{B}_{D_{CP-} \rightarrow l}} \right). \quad (9)$$

As for the  $\delta_{K\pi}$  analysis, the branching fractions can be measured as:

$$\mathcal{B}_{D_{CP+} \rightarrow l} = \frac{n_{l;CP\pm}}{n_{CP\pm}} \cdot \frac{\epsilon_{l;CP\pm}}{\epsilon_{CP\pm}}, \quad (10)$$

where  $n_{CP\pm}$  ( $n_{l;CP\pm}$ ) and  $\epsilon_{CP\pm}$  ( $\epsilon_{l;CP\pm}$ ) denote the signal yields and detection efficiencies of ST mode (DT of  $D\bar{D} \rightarrow l; CP\pm$ ).

In this analysis [14], we use 3  $CP$ -even ( $K^+K^-$ ,  $\pi^+\pi^-$ ,  $K_S^0\pi^0\pi^0$ ) and 3  $CP$ -odd ( $K_S^0\pi^0$ ,  $K_S^0\omega$ ,  $K_S\eta$ ) tag modes, and the semileptonic decays used for the DT are  $K^\mp e^\pm \nu_e$  plus  $K^\mp \mu^\pm \nu_\mu$ . We use the  $M_{BC}$  and  $\Delta E$  to select a fully reconstructed  $D$  candidate in the ST sample. In each ST event, we search for semileptonic  $D \rightarrow Ke(\mu)\nu$  candidates using the unpaired tracks. We define the variable  $U_{miss}$  to distinguish signals from backgrounds:

$$U_{miss} \equiv E_{miss} - c|\vec{p}_{miss}|$$

$$E_{miss} \equiv E_0 - E_K - E_l, \quad |\vec{p}_{miss}| \equiv - \left[ \vec{p}_K + \vec{p}_l + \hat{p}_{ST} \sqrt{E_0^2 + m_D^2} \right], \quad (11)$$

where  $E_{K,l}$  ( $\vec{p}_{K,l}$ ) is the energy (three-momentum) of  $K$  ( $l$ ),  $\hat{p}_{ST}$  is the unit vector in the direction of the reconstructed  $CP$ -tagged  $D$ , and  $m_D$  is the nominal  $D^0$  mass [6]. The  $U_{miss}$  distributions for correctly-reconstructed signal peak at zero, and in Fig. 2 are reported, for example, the distributions for the  $D\bar{D} \rightarrow Ke\nu_e$ ;  $K^+K^-$  and  $D\bar{D} \rightarrow K\mu\nu_\mu$ ;  $K^+K^-$  modes.

In the fits of the DT  $Ke\nu_e$  modes, the signal shape is modeled using MC shape convoluted with a bifurcated Gaussian, while the background is described with a 1st-order polynomial function. For the  $K\mu\nu_\mu$  modes, the signal shape is modeled using the same functions as for the  $Ke\nu_e$  modes. However, the background is more complex and consist of three parts. Primary background comes from  $D \rightarrow K\pi\pi^0$  events. The background shape is taken from a  $K\pi\pi^0$  MC control sample and corrected for the data/MC efficiency resolution. The size of the  $K\pi\pi^0$

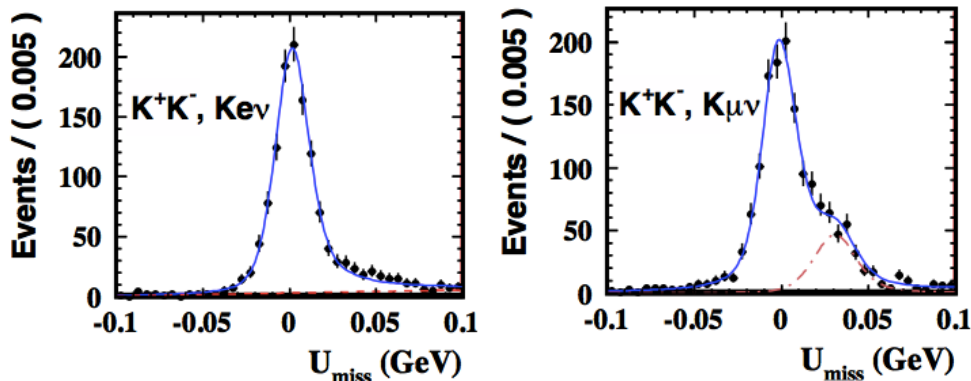


**Figure 2.**  $U_{miss}$  distributions and fits to data for the  $CP$ -tagged  $Ke\nu_e$  (left) and  $K\mu\nu_\mu$  (right) DT samples. In each plot, the solid line is the total fit, the dashed line in  $Ke\nu$  is the polynomial background contribution, and the dotted dashed line in  $K\mu\nu$  represents the contribution from the  $K\pi\pi^0$  background.

background is then fixed by scaling the number of  $K\pi\pi^0$  events in the control sample to the number in the signal region according to the simulated relative efficiencies of the selection criteria. The second background component from  $Ke\nu$  events in  $K\mu\nu$  mode is well modeled using MC events. All the other backgrounds are described with a first-order polynomial function.

To combine the results from different  $CP$  modes, we use the standard weighted-last square method [6]. The weighted semileptonic branching fraction  $\tilde{\mathcal{B}}_{DCP\pm\rightarrow l}$  is determined by minimizing the quantity:  $\chi^2 = \sum_a (\tilde{\mathcal{B}}_{DCP\pm\rightarrow l} - \mathcal{B}_{DCP\pm\rightarrow l}^\alpha) / (\sigma_{CP\pm}^\alpha)^2$ , where  $\alpha$  denotes the different  $CP$ -tag modes, and  $\sigma_{CP\pm}^\alpha$  is the statistical error of  $\mathcal{B}_{DCP\pm\rightarrow l}^\alpha$  for a given  $\alpha$ . Using this  $\tilde{\mathcal{B}}$  in Eq. (9), we obtain [14]

$$y_{CP} = (-2.0 \pm 1.3 \pm 0.7)\%,$$

where the quoted uncertainties are statistical and systematic, respectively.

This result is compatible with previous measurements [10, 12, 15] within  $2\sigma$ , and is the most precise time-integrated measurement of  $y_{CP}$  at charm threshold.

## 5. Observation of $Z_c$ states at BESIII

One of the physics goal of the BESIII experiment is the study of the charmonium-like states:  $X$ ,  $Y$ , and  $Z$  states. In particular, in this second part we report a summary on the four  $Z_c$  states observed in the last two years:  $Z_c(3900)$ ,  $Z_c(4020)$ ,  $Z_c(3885)$ , and  $Z_c(4025)$ . These states have at least four quarks, carry electric charge, and are close to the threshold.

### 5.1. Discovery of $Z_c(3900)^+$

In the study of the process  $e^+e^- \rightarrow J/\psi\pi^+\pi^-$ , using a data sample of  $525 \text{ pb}^{-1}$  collect at  $\sqrt{s} = 4.260 \text{ GeV}$  with the BESIII detector, we observe a peaking structure in the invariant  $J/\psi\pi^\pm$  mass distribution [16], with a statistical significance larger than  $8\sigma$ . This structure, called  $Z_c(3900)$  state, is parameterized with a S-wave Breit-Wigner function convoluted with a function accounting for the detector resolution. The fit result is shown in Fig. 3, and the mass and width obtained from the fit are  $(3899.0 \pm 3.6(\text{stat.}) \pm 4.9(\text{syst.})) \text{ MeV}/c^2$  and  $(46 \pm 10(\text{stat.}) \pm 20(\text{syst.})) \text{ MeV}$ , respectively. The  $Z_c(3900)^+$  state was almost simultaneously observed by the Belle collaboration [17] and then confirmed by CLEO-c [18].

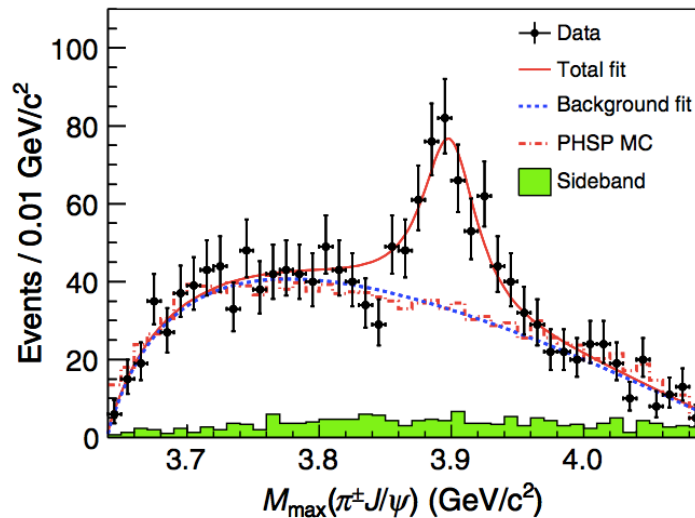


**Figure 3.** Fit to the  $M_{max}(J/\psi\pi)$  distribution, where  $M_{max}$  stands for the larger of the two mass combinations  $M(J/\psi\pi^+)$  and  $M(J/\psi\pi^-)$  in each event. Dots with error bars are data, red solid line shows the fit result, and the blue dotted line the background. In the figure are also reported the results of a phase space MC simulation (dotted-dashed histogram), and the normalized  $J/\psi$  sideband events.

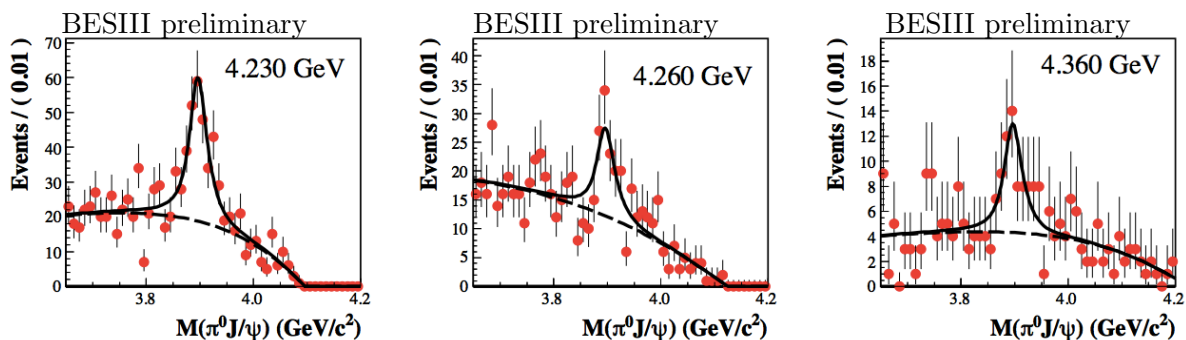


**Figure 4.** Invariant  $J/\psi$  mass spectra for  $e^+e^- \rightarrow J/\psi\pi^0\pi^0$  at  $\sqrt{s} = 4.23$  GeV (left), 4.26 GeV (middle), and 4.36 GeV (right). Data are represented by the red points with error bars, while solid black line shows the fit fit results and the dashed line the background contribution.

Since the  $Z_c(3900)$  couples to a  $c\bar{c}$  state and carry electric charge, it should be a tetraquark state, as well as a hadronic molecule, or other configuration. In addition, it should be noted that it is very close to the  $D\bar{D}^*$  threshold, and this might be related to its nature.

A very recent BESIII analysis search for the neutral isospin partner of  $Z_c(3900)^\pm$ . Evidence for a structure in the invariant  $J/\psi\pi^0$  mass distribution is observed in CLEO-c data [18] in the process  $e^+e^+ \rightarrow J/\psi\pi^0\pi^0$ . We study the same channel at three different c.m. energies,  $\sqrt{s} = 4.23, 4.26,$  and  $4.36$  GeV, and we observe a clear structure in the invariant  $J/\psi\pi^0$  mass, as shown in Fig. 4, where the preliminary results are reported. We fit the signal with a Breit-Wigner function and we found a mass and width values of  $(3894.8 \pm 2.3)$  MeV/ $c^2$  and  $(29.6 \pm 8.2)$  MeV, respectively, where the quoted error is statistical only. This result is consistent with the value obtained for the charged  $Z_c(3900)^+$  and with the value reported in Ref. [18]. However, the

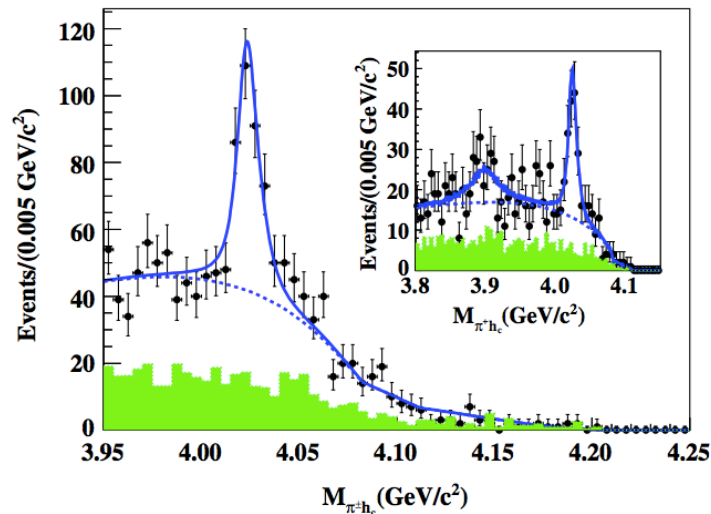


**Figure 5.** Sum of simultaneous fit to the  $M_{h_c\pi^\pm}$  distribution at  $\sqrt{s} = 4.23, 4.26,$  and  $4.36$  GeV. In the inset is reported the distribution at  $4.23$  and  $4.26$  GeV including the  $Z_c(3900)$ . Solid line represents the total fit, dashed line the background contribution. Data are represented by points with error bars, and shaded histograms are the normalized sideband background.

determination of the spin-parity of the  $Z_c(3900)^+$  and  $Z_c(3900)^0$  states is necessary to confirm if the two states establish an isospin triplet.

### 5.2. Observation of the $Z_c(4020)$

The process  $e^+e^- \rightarrow h_c\pi^+\pi^-$  is studied at 13 different c.m. energies from 3.90 to 4.42 GeV. A charged structure is observed in the  $h_c\pi^\pm$  invariant mass spectrum at  $4.02$   $\text{GeV}/c^2$  [19], very close to the  $D^*\bar{D}^*$  threshold. This structure is called  $Z_c(4020)$  hereafter. In this study, we reconstruct the  $h_c$  via its electric-dipole transition  $h_c \rightarrow \gamma\eta_c$ , with the  $\eta_c$  reconstructed in 16 exclusive hadronic final states.

In Fig. 7 is shown the fit result to the  $h_c\pi^\pm$  mass spectrum obtained by fitting the data at  $4.23, 4.26$  and  $4.36$  GeV simultaneously with the same signal function with common mass and width. The signal shape is parameterized as a constant width relativistic Breit-Wigner function convoluted with a Gaussian with a mass resolution determined from data, while the background shape is parameterized as an ARGUS function. The mass and width from the fit are  $(4022.9 \pm 0.8 \text{ MeV}/c^2)$  and  $(7.9 \pm 2.7) \text{ MeV}$ , respectively, and the statistical significance of the  $Z_c(4020)$  signal is calculated to be greater than  $8.9\sigma$ . There is no significant evidence of the  $Z_c(3900)$  structure in the  $M_{h_c\pi^\pm}$  mass spectrum: adding the  $Z_c(3900)$  mass and width fixed to the BESIII measurement [16], we find a significance of  $2.1\sigma$ .

A neutral structure,  $Z_c(4020)^0$ , is expected to couple to the  $h_c\pi^0$  final state and to be produced in the process  $e^+e^- \rightarrow h_c\pi^0\pi^0$ . In the study of this process [20] a significant signal was observed in the  $M_{h_c\pi^0}$  invariant mass distribution at about the same mass value found for the charged  $Z_c(4020)$ . Parameterizing the signal with a Breit-Wigner function and fixing the width to the value extracted from Ref [16], the fit yields a mass of  $(4023.9 \pm 2.2 \pm 3.8) \text{ MeV}/c^2$ , which is consistent with the mass value of the charged  $Z_c(4020)$ . However, also in this case, further investigation are needed to understand the nature of  $Z_c(4020)$ .



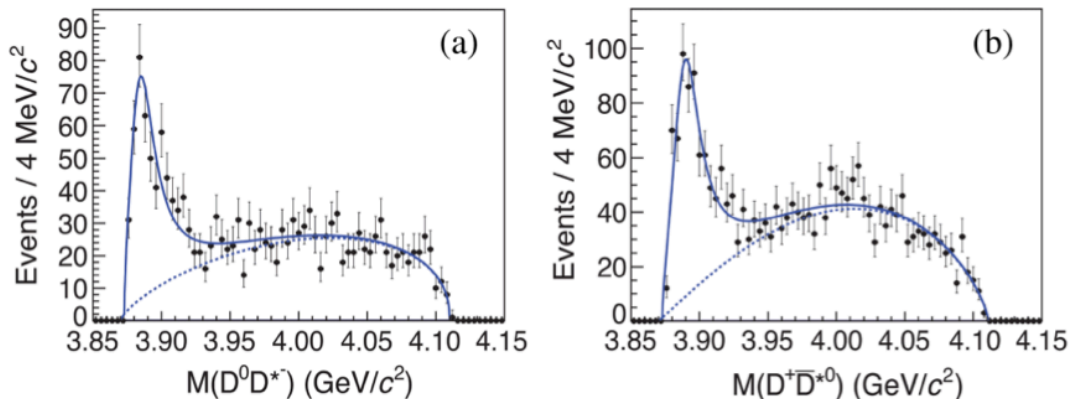


**Figure 6.** Fit to the invariant mass distributions for (a)  $D^0 D^{*-}$  and (b)  $D^+ \bar{D}^{*0}$  events. The dots with error bars are the data, the solid line is the total fit, and dashed line describes the background distribution.

5.3. *Observation of the  $Z_c(3885)$  in the  $D\bar{D}^*$  final state, and  $Z_c(4025)$  in the  $D^* \bar{D}^*$  final state.* Due to the proximity of the  $Z_c(3900)$  and  $Z_c(4020)$  states to the  $D\bar{D}^*$  and  $D^* \bar{D}^*$  threshold, it is also interesting to search for similar structures in the corresponding open charm channels. The comparison between the  $Z_c$  partial decay widths to a  $c\bar{c}$  final state, with the decay widths to a pair of open charm mesons may help to understand their nature. At BESIII, we investigate the processes  $e^+e^- \rightarrow (D\bar{D}^*)^\pm \pi^\mp$  [21], and  $e^+e^- \rightarrow (D^* \bar{D}^*)^\pm \pi^\mp$  [22] at the  $\sqrt{s} = 4.26$  GeV, using a sample of  $525 \text{ fb}^{-1}$  and  $827 \text{ fb}^{-1}$ , respectively. The reactions are partially reconstructed: the bachelor  $\pi^\pm$  is detected, and only one final state  $D$  meson are fully reconstructed. The other  $D$  meson is inferred from energy momentum conservation.

For the  $(D\bar{D}^*)^\pm$  system, we reconstruct the  $D$  meson from  $K\pi$  and  $K\pi\pi$  decays. The invariant mass distribution of the  $(D\bar{D}^*)$  system shows a clear enhancement at the  $(D\bar{D}^*)$  threshold, labeled as  $Z_c(3885)^\pm$  (see Fig. 7). The fit of the enhancement with a Breit-Wigner function yields a mass and width of  $(3883.9 \pm 1.5 \pm 4.2) \text{ MeV}/c^2$  and  $(24.8 \pm 3.3 \pm 11.0) \text{ MeV}$ , respectively. The bachelor  $\pi^\pm$  angle distribution is analyzed in order to determine the  $Z_c(3885)$  quantum number. The resulting distribution is consistent with a spin-parity assignment of  $J^P = 1^+$ , and rules out  $0^-$  as well as  $1^-$ . A new preliminary analysis, which uses more statistics and a double-tag technique, improves and confirms the results obtained in Ref. [21]. An important question is whether or not the  $Z_c(3900)$  and  $Z_c(3885)$  have the same origin. The determination of the  $J^{PC}$  quantum number of  $Z_c(3900)$  would be necessary to unswear this question. However, if we assume that the  $Z_c(3885)$  structure is due to the  $Z_c(3900)$ , the ratio of partial decay width is determined to be  $\Gamma(Z_c(3885) \rightarrow D\bar{D}^*)/\Gamma(Z_c(3900) \rightarrow J/\psi\pi) = 6.2 \pm 1.1 \pm 2.7$ , which is much smaller than typical values for decays of conventional charmonium states above the open charm threshold. The comparison between mass, width, and cross section is reported in Table ?? for the  $Z_c(3900)^\pm$  and  $Z_c(3885)^\pm$  states.

For the  $e^+e^- \rightarrow (D^* \bar{D}^*)^\pm \pi^\mp$  process, the charged  $D$  meson from  $D^{*\pm} \rightarrow D^\pm \pi^0$  is reconstructed by its decay into  $K\pi\pi$ , and at least one  $\pi^0$  in the final state is required in order to suppress background events. In the recoil mass spectrum of the bachelor  $\pi^\mp$ , a structure near the  $(D^* \bar{D}^*)^\pm$  threshold is observed. We assume that this enhancement is due to a particle, labeled as  $Z_c(4025)$ , and we fit the distribution with a Breit-Wigner function, as shown in Fig. 7. The fit yields a mass of  $(4026.3 \pm 2.6 \pm 3.7) \text{ MeV}/c^2$  and a width of  $(24.8 \pm 5.6 \pm 7.7) \text{ MeV}$ . Unfortunately, the statistics do not allow to perform a spin-parity analysis of  $Z_c(4025)$ , and

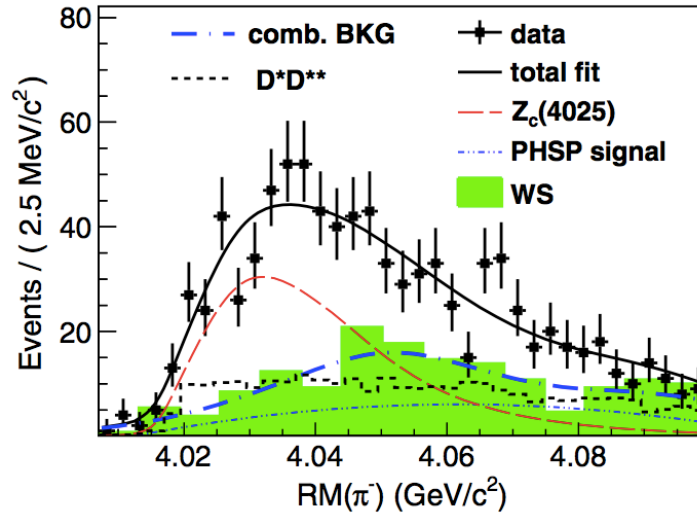


**Figure 7.** Unbinned maximum likelihood fit to the  $\pi^-$  recoil mass spectrum. Points with error bars are the data, solid line is the best fit result. Backgrounds,  $Z_c(4025)^+$  signal, and phase space signal component (PHSP) are also shown.

	$Z_c(3885) \rightarrow D\bar{D}^*$	$Z_c(3900) \rightarrow J/\psi\pi$
Mass ( $\text{MeV}/c^2$ )	$3883.9 \pm 1.5 \pm 4.2$	$3899.0 \pm 3.6 \pm 4.9$
Width (MeV)	$24.8 \pm 3.3 \pm 11.0$	$46 \pm 10 \pm 20$
$\sigma \times \mathcal{B}$ (pb)	$83.5 \pm 6.6 \pm 22.0$	$13.5 \pm 2.1 \pm 4.8$

**Table 1.** Masses, widths and product of the Born cross sections times branching fractions for  $Z_c(3885)$  [21] and  $Z_c(3900)$  [16].

	$Z_c(4025) \rightarrow D^*\bar{D}^*$	$Z_c(4020) \rightarrow h_c\pi$
Mass ( $\text{MeV}/c^2$ )	$4026.3 \pm 2.6 \pm 3.7$	$4022.9 \pm 0.8 \pm 2.7$
Width (MeV)	$24.8 \pm 5.6 \pm 7.7$	$7.9 \pm 2.7 \pm 2.6$
$\sigma$ (pb)	$139 \pm 9 \pm 15$	$8.7 \pm 1.9 \pm 2.8 \pm 1.4$ at $\sqrt{s} = 4.23$ GeV
		$7.5 \pm 1.7 \pm 2.1 \pm 1.2$ at $\sqrt{s} = 4.26$ GeV
		$10.3 \pm 2.3 \pm 3.1 \pm 1.6$ at $\sqrt{s} = 4.36$ GeV

**Table 2.** Masses, widths and Born cross sections for  $Z_c(4025)$  [22] and  $Z_c(4020)$  [19].

also in this case further investigation of the  $Z_c(4020)$  and  $Z_c(4025)$  are mandatory in order to understand if whether or not both are due to the same source. Table 2 summarizes the mass, width and cross section for the  $Z_c(4020)^\pm$  and  $Z_c(4025)^\pm$  states.

## 6. Conclusions

Using a data sample of  $2.92 \text{ fb}^{-1}$  collected with the BESIII detector at  $\sqrt{s} = 3.773$  GeV, we measure the strong phase  $\cos \delta_{K\pi}$  and the mixing parameter  $y_{CP}$  exploiting a quantum-correlated technique. We found  $\cos \delta_{K\pi} = 1.02 \pm 0.11 \pm 0.06 \pm 0.01$  and  $y_{CP} = (-2.0 \pm 1.3 \pm 0.7)\%$ , where the first uncertainty is statistical, the second systematic, and the third is due to the external input parameters. Despite the current precision is statistically limited, these are the most precise time-

integrated measurements at charm threshold. Future efforts, both in the global fit procedure than in the data taking, will be implemented in order to reduce the statistical uncertainty by a factor two.

Recent studies focalize the efforts in the charmonium mass region. In particular, four charged and two neutral charmonium-like states have been observed,  $Z_c(3885)^\pm$ ,  $Z_c(3900)^\pm$ ,  $Z_c(3900)^0$ ,  $Z_c(4020)^\pm$ ,  $Z_c(4020)^0$ ,  $Z_c(4025)^\pm$ : these states may be an indication of a new type of hadrons. In the near future, BESIII experiment will take more data in the  $XYZ$  region, which will be helpful to shed light on the nature of these new states.

## References

- [1] Glashow S L, Iliopoulos J and Maiani L 1970 *Phys. Rev. D* **2**(7) 1285–1292
- [2] Cabibbo N 1963 *Phys. Rev. Lett.* **10**(12) 531–533
- [3] Kobayashi M and Maskawa T 1973 *Prog.Theor.Phys.* **49** 652–657
- [4] Aaij R *et al.* ((LHCb Collaboration)) 2013 *Phys. Rev. Lett.* **110**(10) 101802
- [5] Aaltonen T *et al.* ((CDF Collaboration)) 2013 *Phys. Rev. Lett.* **111**(23) 231802
- [6] Olive K *et al.* (Particle Data Group) 2014 *Chin.Phys.* **C38** 090001
- [7] del Amo Sanchez P *et al.* (BABAR Collaboration) 2010 *Phys. Rev. Lett.* **105**(8) 081803
- [8] Staric M (Belle Collaboration) 2012 (*Preprint 1212.3478*)
- [9] Ablikim M *et al.* ((BESIII Collaboration)) 2010 *Nucl. Instrum. Meth. A* **614** 345 – 399 ISSN 0168-9002
- [10] Asner D M *et al.* (CLEO Collaboration) 2012 *Phys. Rev. D* **86**(11) 112001
- [11] Xing Z Z 1997 *Phys. Rev. D* **55**(1) 196–218
- [12] Y. Amhis *et al.* (Heavy Flavor Averaging Group) (2012), arXiv:1207.1158 and online update <http://www.slac.stanford.edu/xorg/hfag/osc/spring.2014/> accessed: 2010-09-30
- [13] Ablikim M *et al.* (BESIII Collaboration) 2014 *Physics Letters B* **734** 227 – 233 ISSN 0370-2693
- [14] Ablikim M *et al.* (BESIII Collaboration) 2015 (*Preprint 1501.01378*)
- [15] Lees J P *et al.* (BaBar Collaboration) 2013 *Phys. Rev. D* **87**(1) 012004
- [16] Ablikim M *et al.* (BESIII Collaboration) 2013 *Phys. Rev. Lett.* **110**(25) 252001
- [17] Liu Z Q *et al.* (Belle Collaboration) 2013 *Phys. Rev. Lett.* **110**(25) 252002
- [18] Xiao T, Dobbs S, Tomaradze A and Seth K K 2013 *Physics Letters B* **727** 366 – 370 ISSN 0370-2693
- [19] Ablikim M *et al.* 2013 *Phys. Rev. Lett.* **111**(24) 242001
- [20] Ablikim M *et al.* ((BESIII Collaboration)) 2014 *Phys. Rev. Lett.* **113**(21) 212002
- [21] Ablikim M *et al.* ((BESIII Collaboration)) 2014 *Phys. Rev. Lett.* **112**(2) 022001
- [22] Ablikim M *et al.* ((BESIII Collaboration)) 2014 *Phys. Rev. Lett.* **112**(13) 132001